*Proceedings of the 9th World Congress on Mechanical, Chemical, and Material Engineering (MCM'23)*
*Brunel University, London, United Kingdom –August 06-08, 2023*
*Paper No. HTFF 191*
*DOI: 10.11159/htff23.191*

# A GPU-Accelerated Hydrodynamics Solver for Atmosphere-Fire Interactions

**Jhamieka Greenwood[1], Dr. Bryan Quaife[2]**
[1, 2] Florida State University, Department of Scientific Computing
Tallahassee, FL, US
jgreenwood@fsu.edu; bquaife@fsu.edu

***Abstract*** - A fundamental process to understand fire spread is it's coupling with the atmospheric flow. Building computational tools to simulate this complex flow has several challenges including boundary layer effects, resolving vegetation and the forest canopies, and conserving fluid mass. We develop a two-dimensional hydrodynamic solver that models fire-induced flow as a convective sink that converts the two-dimensional horizontal flow into a vertical flow through the buoyant plume. The resulting equations are the two-dimensional Navier-Stokes equations, but with a point-source delta function appearing in the conservation of mass equation. We develop a projection method to solve these equations and implement them on a GPU architecture. The ultimate goal is to simulate wildfire spread faster than real-time, and with the ability for users to introduce real-time updates in an augmented reality sandbox.

***Keywords*****:** computational fluid dynamics, fire dynamics, Navier-Stokes, prescribed fire

## 1. Introduction

We live in a time when we see the effects of climate change daily. We are experiencing temperature increases, precipitation decreases, and low humidity levels. The high temperatures and low relative humidity are key to wildfire ignition and spread [1]. These factors can be seen from the relationship between the observed climate and the burned area over the last 100 years [1]. Global climate models can make future projections based on historical data. Future projections predict increased global temperature ranging from 2.0 to 2.6 °C for mid-century (2036 to 2065) and 2.8 to 4.6 °C for the end of the century (2071 to 2100), depending on future greenhouse gas emissions [2]. Increased global temperatures can decrease fuel moisture and increase the duration of warm, dry weather, creating large areas of dry fuels that are more likely to ignite and carry fire over a longer period [2]. These conditions are prominent during peak wildfire season. The National Significant Wildland Fire Potential Outlook report predicts above-normal significant fire potential for Florida, most of the Southwest, northern California, the southern High Plains, the southern Great Basins, central to southwest Oregon, central Washington, and much of the Northwest during the summer months from May to August [3]. This prediction directly corresponds with one of the significant factors responsible for wildfires, lightning strikes, which is responsible for one-third of the forest fires from May to September each year and is also associated with global warming [1]. Due to decreased fuel moisture and increased temperatures, one can see how these conditions and factors can contribute to destructive wildfires.

There is an unprecedented need for more ways to increase predictability and mitigate wildfire risks. One way is to understand the behavior of wildfires through the permutations of fuels, weather, and topography. Each component has numerous characteristics that affect how fires behave, that is, how they spread and release energy [4]. This work investigates the fundamental processes critical to fire spread, which involve many factors and complex processes. It focuses on the complex coupling of the combusting environment and the atmospheric flow. In particular, what variables influence fire-induced flows, and how do they contribute to fire spread?

We use the fundamental equations describing fluid motions to describe fire-atmospheric coupling. These models describe the air permeating around a fire to study the cycling airflow that pulls air into the burning. We explore how air particles are transported around the fire, tracking through movements in space and time. More importantly, we study how the wind affects fire spread by acting as an external force. In summary, the model introduces a novel approach to model the conversion of two-dimensional horizontal momentum into vertical momentum through a buoyant plume. In addition, the

model will be an operational tool for fire scientists to study the spread of fire and further understand the behavior of prescribed fires and wildfires.

## 2. Related Work

Computational fluid dynamics (CFD) simulations have a history dating back to the early 1970s, with uses in aerospace, oceanography, architecture, and computer graphics. In modern computer graphics, we use CFD simulations to develop fluid-like behaviors. In the special effects industry, there is a high demand to convincingly mimic the appearance and behavior of fluids such as smoke, water, and fire [5]. Most fluid flow of interest in computer graphics is governed by the incompressible Navier-Stokes equations, a set of partial differential equations that are assumed to hold throughout the fluid [6]. The simulation in this work is based on the Stable Fluids solver by Jos Stam, where he proposes a stable algorithm that solves the full Navier-Stokes equations [5].

Scientific investigation of wildfires in the early 1900s was driven by the need for predictive tools to support planning efforts and operational decisions that were both tactical and strategic [4]. Fire dynamics and the scientific study of wildfire behavior refers to the empirical and semi-empirical models based on Richard C. Rothermal's mathematical model for predicting fire spread. In the last century, there has been an influx of computational fluid dynamics models to bolster these investigations, with some using his model. In 1997, Rodman Linn developed a coupled atmospheric transport/wildfire behavior model at Los Alamos National Laboratory, FIRETEC [7]. At the Los Alamos National Laboratory, scientists developed robust physics-based 3-D computer programs to simulate the relationship between fire and its environment. HIGRAD is a CFD model that investigates atmosphere-fire interactions in the presence of various fuel types. FIRETEC studies the physics components of combustion, heat transfer, and turbulence. However, FIRETEC is performed on the computer processing unit (CPU) using OpenMP as the parallelization API. The initial FIRETEC model described an enormous set of chemical reactions simplified to a small set of reactions involving wood pyrolysis and several solid-gas and gas-gas reactions [7]. FIRETEC has been combined with the hydrodynamic model HIGRAD to simulate wildfires using a terrain following a three-dimensional finite volume grid [7]. HIGRAD explicitly solves the compressible Navier-Stokes equations in arbitrarily complex, three-dimensional Cartesian geometry, including atmospheric and topographic effects at the wind plant scale [8]. This combination allows scientists to study wildfire behavior rendering the realistic topology of the terrain and weather effects.

Studying fire at landscape levels helps researchers and land managers manage operations and create plans to mitigate wildfire risks. FARSITE was one of the first models to integrate aspects of established individual fire behavior [9]. The simulator incorporates fire behavior models from the spread of various fire ignition patterns and fuel moisture, demonstrating the links between existing fire behavior models and the consequences to spatial patterns of fire growth and behaviour [9]. However, as fire science has evolved, models such as FARSITE do not consider that weather, fuel characteristics, and topography are not independent influences. Weather affects wildfires through fuel and terrain by controlling the fuel moisture through precipitation, ambient relative humidity, and increased evaporation driven by winds and complicating the fire-spread-accelerating effect of steep slopes with topographically induced accelerations [10]. Kinematic models such as FARSITE are limited when considering the rate of spread and the production of fire-induced flows.

When investigating a fire’s evolution, it is crucial to study the dynamic forces between the external environment factors that affect wildland fires: weather, fuel characteristics, and topography [10]. Coupled weather-wildland fire models such as WRF-Fire and the Coupled Atmosphere-Wildland Fire-Environment (CAWFE), aim not only to simulate the direction and rate of fire spread but to describe interacting dynamical forces, reproduce characteristic phenomena, and provide an understanding of why each fire unfolds in the unique way that it does [11]. WRF-Fire and CAWFE are prediction models that couple a numerical weather prediction (NWP) model with a wildland fire behavior module representing the growth of a fire propagating through surface fuels and highlight the dynamic exchange of forces

between the fire and its atmospheric environment [10]. Both models emphasize the importance of considering NWP models and their attributes in wildland fire research. The simulation in this work is inspired by CFD models in fire science. It focuses on the fire-induced flows as a convective sink that converts the two-dimensional horizontal flow into a vertical flow through the buoyant plume. The main contribution of this work is to provide additional understanding of the atmospheric flow around the ignition site of a fire and the unique effects during a wildland fire event. To investigate another approach, Jason Sharples used WRF-Fire to understand the pyro-convection phenomena of vorticity-driven lateral fire spread (VLS). This approach examines the sensitivity of resolving VLS to horizontal and vertical grid spacing and fire-to-atmosphere coupling within the model framework [12]. The lateral fire spread, driven by fire whirls, formed due to an interaction between the background winds and the vertical circulation generated at the flank of the fire front as part of the pyro-convective updraft [12]. Sharples concludes that with VLS, the laterally advancing fire fronts become the dominant contributor to the power of the fire [12]. Through the research mentioned above, there are many ways to approach the problem of how fire spreads. The goal of this work is to present another one.

## 4. Overview of Equations

In this paper, the Navier-Stokes equations are the governing equations used to describe the motion of the atmospheric flow

$$\frac{\partial \mathbf{u}}{\partial t} = -(\mathbf{u}\cdot\nabla)\mathbf{u} - \frac{1}{\rho}\nabla \mathrm{p} + \nu\nabla^2\mathbf{u} + \mathbf{f}, \tag{4.1}$$

$$\nabla\cdot\mathbf{u} = 0, \tag{4.2}$$

where **u** is the velocity field, $t$ is time, $\rho$ is the density, p is the pressure, $\nu$ is the kinematic viscosity, and **f** is the external force. These equations are supplemented with periodic boundary conditions and an initial condition.

The Navier-Stokes equations are obtained by imposing that the fluid conserves both mass (4.2) and momentum (4.1) [5]. However, we modify the mass equation to simulate a buoyant plume at the locations $\boldsymbol{x}_i = 1, \ldots, \mathbf{N}$, where **N** is number of points in the domain, and conserving mass in the remaining domain of the velocity field. That is,

$$\nabla\cdot\mathbf{u} = -\sum_{i=1}^{N} Q\delta(\boldsymbol{x}-\boldsymbol{x}_i). \tag{4.3}$$

where $\delta$ is a point-source delta function and Q is the rate that depends on fire intensity. Using the Dirac mass, $\delta$, is a novel approach to model the conversion of two-dimensional horizontal momentum into vertical momentum through a buoyant plume.

We developed a projection method similar to Chorin's classical method. We use the *Helmholtz-Hodge Decomposition* theorem to write the solution of (4.1) as

$$\mathbf{u} = \mathbf{w} - \nabla \mathrm{q} \tag{4.4}$$

where **w** has divergence at $\boldsymbol{x}_0$ and zero divergence everywhere else, and q is a scalar field [13]. Using this theorem and modifying the mass equation leads to a new projection operator, **P**, which projects any vector field **u** onto its divergence-free field with convective sinks. The projection operator is $\boldsymbol{u} = \boldsymbol{P}\boldsymbol{w} := \boldsymbol{w} - \nabla q$, where

$$\nabla^2 \mathrm{q} = \nabla \cdot \mathbf{w} + \sum_{i=1}^{N} \delta(\boldsymbol{x} - \boldsymbol{x}_i). \tag{4.5}$$

Equation (4.5) is a Poisson equation for the scalar field q, where q is periodic on $\partial D$ [5]. We solve the equation by writing q as the sum of the fundamental solution of the Laplacian, Δ, centered at $\boldsymbol{x}_i$, and a regularization term that satisfies Laplace's equation.

$$\mathbf{u} = \mathbf{w} - \nabla \mathrm{q} + \frac{Q}{\pi} \sum_{i=1}^{N} \frac{(\boldsymbol{x} - \boldsymbol{x}_i)}{|\boldsymbol{x} - \boldsymbol{x}_i|^2 + \varepsilon^2} \tag{4.6}$$

where $\varepsilon \ll 1$ is a regularization parameter. We modify Jos Stam's stable fluid solver and the resulting method is

$$\frac{\partial \mathbf{u}}{\partial t} = \mathbf{P}(-(\mathbf{u} \cdot \nabla)\mathbf{u} + \nu \nabla^2 \mathbf{u} + \mathbf{f}) - \frac{1}{\pi \rho} \sum_{i=1}^{N} \frac{(\boldsymbol{x} - \boldsymbol{x}_i)}{|\boldsymbol{x} - \boldsymbol{x}_i|^2 + \varepsilon^2}, \tag{4.7}$$

$$\nabla \cdot \mathbf{u} = -\sum_{i=1}^{N} Q \delta(\boldsymbol{x} - \boldsymbol{x}_i). \tag{4.8}$$

## 5. Implementation Pipeline

The fluid solver in this work iterates through six steps: introduce a force, advect the velocity with a Semi-Lagrangian method, diffuse the velocity with a Fourier method, project the results of the velocity field that satisfies the modified mass equation (4.3), normalize the velocity field, add convective sinks, and prepare each particle for texture mapping. The method is solved by sequentially iterating these steps over the span of $\Delta t$, a time step. We resolved each term on the right-hand side of equation (4.1) while satisfying equation (4.3).

In this interactive system, forces are only applied at the beginning of each time step, starting with an initial state $\boldsymbol{u}_o = \boldsymbol{u}(\boldsymbol{x}, 0)$ [5]. The fourth term of equation (4.1) encapsulates acceleration due to an external force applied to the fluid [14]. The force manipulates the fluid to behave in some way. In the context of studying wildfire behavior, this action is the force from wind or airflow around a fire

$$\boldsymbol{u}_1(\mathbf{x}) = \mathbf{u}_0(\mathbf{x}) + \Delta \mathrm{t} \mathbf{f}(\mathbf{x}, \mathrm{t}). \tag{5.1}$$

The force vector, **f**, is calculated from motion coordinates multiplied by a force scale factor, $\Delta t$, and a force fall function $(1 + \boldsymbol{x}^4 + \boldsymbol{y}^4)^{-1}$ for smoothness. This approach is identical to the one used by Stam [5].

Once a force is applied, the velocity is advected with the velocity field, **u**. A disturbance somewhere in the fluid propagates according to the expression $-(\boldsymbol{u} \cdot \nabla)\boldsymbol{u}$ [5]. This expression is the first term in equation (4.1). As the particles move through the fluid at each time step, the velocity at the new position **x** at time $t + \Delta t$ is backtracked through the velocity field and set to the current position **x**.

$$\boldsymbol{u}_2(\mathbf{x}) = \mathbf{u}_1\big(\mathbf{p}(\mathbf{x}, -\Delta \mathrm{t})\big), \tag{5.2}$$

where p is a characteristic. The Semi-Lagrangian method uses an Eulerian grid and interpolate to Lagrangian points with a bilinear interpolator. Again, this approach is identical to Stam's [5].

The fluid viscosity is incorporated by solving

$$\frac{\partial \boldsymbol{u}_2}{\partial t} = \nu \nabla^2 \boldsymbol{u}_2. \tag{5.3}$$

with the implicit method [5]

$$(\mathbf{I} - \nu \Delta t \nabla^2)\boldsymbol{u}_3(\mathbf{x}) = \mathbf{u}_2(\boldsymbol{x}). \tag{5.4}$$

Again, this is the same approach taken by Stam [5].

We perform diffusion and projection methods in the frequency domain by using the cuFFT library. The projection step uses the modified Poisson solver, equations (5.5) and (5.6), utilizing the sparse linear system and projecting onto a new velocity field.

$$\nabla^2 \mathrm{q} = \nabla \cdot \boldsymbol{u}_3 + \sum_{i=1}^{N} \delta(\boldsymbol{x} - \boldsymbol{x}_i). \tag{5.5}$$

$$\mathbf{u}_4 = \boldsymbol{u}_3 - \nabla \mathrm{q} + \frac{Q}{\pi} \sum_{i=1}^{N} \frac{(\boldsymbol{x} - \boldsymbol{x}_i)}{|\boldsymbol{x} - \boldsymbol{x}_i|^2 + \varepsilon^2} \tag{5.6}$$

Using the newly projected velocity field, the convective sink method takes **x** to set the position for the diverging sink.

$$\mathbf{u}_5(\mathbf{x}) = \boldsymbol{u}_4(\mathbf{x}) - \frac{Q}{\pi} \sum_{i=1}^{N} \frac{(\boldsymbol{x} - \boldsymbol{x}_i)}{|\boldsymbol{x} - \boldsymbol{x}_i|^2 + \varepsilon^2} \tag{5.7}$$

The final method updates the particles, **part**, by moving positions according to the velocity field and time. After the particles are updated, each particle is mapped to a texture object and bound for visualization.

$$\mathbf{part}(t+1) = \mathbf{part}(t) + \Delta t \mathbf{u}_5(\mathbf{part}(t)). \tag{5.8}$$

## 6. Periodic Boundaries

The regularized convective sink term in equation (5.7) is not periodic. Since we assume periodic boundaries, this will result in oscillations that will pollute the simulations.

To correct the issue, we include a hyperbolic tangent function to the convective sink method

$$\mathbf{u}(\mathrm{x}) = \frac{(\boldsymbol{x} - \boldsymbol{x}_i)}{|\boldsymbol{x} - \boldsymbol{x}_i|^2 + \varepsilon^2} \cdot \chi(|\boldsymbol{x} - \boldsymbol{x}_i|), \tag{6.0}$$

$$\chi(\mathbf{z}) = -\frac{1}{2}\tanh\big(\alpha(\boldsymbol{z} - \beta)\big) + \frac{1}{2}. \tag{6.1}$$

In equation (6.1), $\alpha$ controls how quickly the function transitions from 1 to 0, $\beta$ represents the center of the transition region, and **z** represents the solution. The hyperbolic tangent function acts as a smooth cutoff function to maintain stability and periodicity in the solver.

## 7. Results and Discussion

Ignition is a vital step of the fire spread process and the initiation of combustion [4]. This work aims to understand the atmosphere-fire interactions around the combustion sites. Our intention is to observe various flow patterns by simulating the mix of pyrolysate gases with the surrounding air from different ignition fire patterns. Note that these examples do not include any background wind.

Figure 1 shows a point-source fire ignition at the center of the 512 x 512 simulation domain after one second and 34 seconds. The source of the fire is pulling the surrounding particles into the ignition site. The closer the particles are to the ignition site, the faster the particles are pulled in. Another observation of the airflow pattern is that the flow enters the area in an elliptical shape, supporting Pierre de Fermat's and Christiaan Huygens' 'least time' principles when applied to fire spread. When used in the context of fire spread, this means that small point-source fires will expand as independent ellipses [4]. When used in fire modeling, both principles observe elliptical fire spread shapes, and in turn, the airflow patterns mimic the same shape of fire growth.

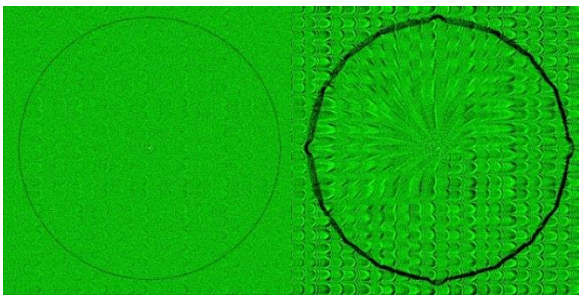

Fig. 1: Simulation results of a point-source fire ignition pattern.

Figure 2 shows a 20-point single-line fire across the center of the 512 x 512 simulation domain after one second and the evolution of the surrounding airflow patterns after 26 seconds. Fire scientists usually use this ignition pattern to observe fires oriented at various angles relative to the wind. In this simulation, no initial wind flow points toward the fire line. However, the convective sinks lead to the development of vortices. As the airflow moves inward toward the center of the fire line, vortex activity increases in four quadrants around the fire line, creating four large eddies.

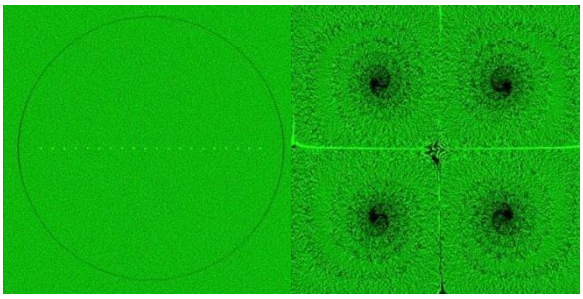

Fig. 2: Simulation results of a line fire ignition pattern.

Figure 3 shows a multi-line V-shaped fire across the center of the 512 x 512 simulation domain after one second and the evolution of the surrounding airflow patterns after 25 seconds. This type of fire ignition pattern develops similar vortex activity as the single-line fire explained above. Two large eddies are produced on the left and right sides of the fire line. Also, an upward-moving airflow appears to be looping due to the periodic boundaries above and below the domain.

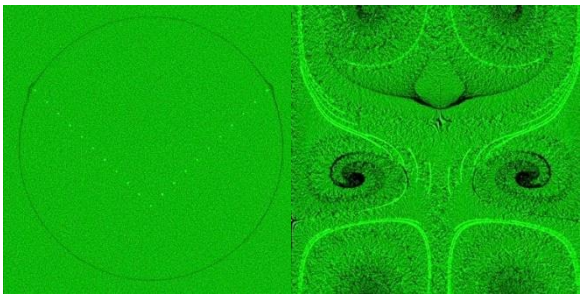

Fig. 3: Simulation results of a V-shaped multi-line fire ignition pattern.

Figure 4 shows a ring fire ignition pattern with no internal ignition after one second and 36 seconds. The circular fire line pulls particles into the ignition sites on all sides, inducing airflow toward the middle of the fire. This fire ignition pattern draws air entrained into the flame zone from the outside towards the middle before substantial outward spread can occur [4]. The fire's inward flow of air and convective heat contributes to developing convective plumes. This indraft towards the center of the fire provides opportunities to lift smoke to high altitudes and offset wind and convective heating on adjacent forest canopies [4].

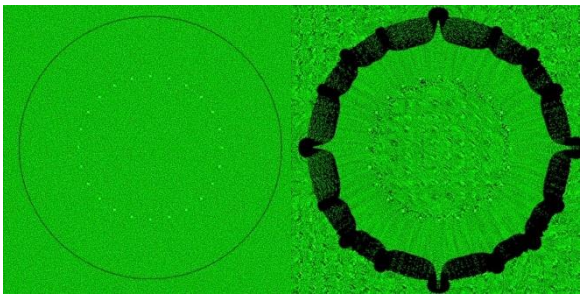

Fig. 4: Simulation results of a ring fire ignition pattern.

## 8. Conclusion

This work introduced a novel approach to solving the Navier-Stokes equations to study fire-induced flows in atmosphere-fire interactions. The program flow was accelerated using CUDA technology on a modern GPU architecture reap the benefits of general-purpose GPU programming. This work provides several examples to demonstrate an view of the fluid simulation's use to investigate wildfire spread. Unlike several other CFD models mentioned in this work, we built the simulation upon a particle simulator using convective sinks as the source of ignition sites. The simulation currently does not have features incorporating temperature, fuels, and topography but has proven to be adequate at modeling fire-inducing flows for fire spread.

## References


[1] S. Mansoor, I. Farooq, M. M. Kachroo, A. E. D. Mahmoud, M. Fawzy, S. M. Popescu, M. Alyemeni, C. Sonne, J. Rinklebe, and P. Ahmad, "Elevation in wildfire frequencies with respect to the climate change," *Journal of Environmental Management,* vol. 301, 2022.

[2] J. E. Halofsky, D. L. Peterson, and B. J. Harvey, "Changing wildfire, changing forests: The effects of climate change on fire regimes and vegetation in the pacific northwest, USA," *Fire Ecology*, vol. 16, no. 1, pp. 1-26, 2020.

[3] *National significant wildland fire potential outlook*, 2022, Predictive Services National Interagency Fire Center.

[4] M. A. Finney, S. S. McAllister, T. P. Grumstrup, and J. M. Forthofer, *Wildland Fire Behaviour: Dynamics, Principles, Processes*, CSIRO Publishing, 2021.

[5] J. Stam, "Stable Fluids," in *Proceedings of the 26th Annual Conference on Computer Graphics and Interactive Techniques,* 1999, pp. 121-128.

[6] R. Bridson, *Fluid Simulations for Computer Graphics*. AK Peters/CRC, 2015.

[7] R. Linn, J. Reisner, J. J. Colman, and J. Winterkamp, "Studying wildfire behaviour using firetec," *International Journal of Wildland Fire*, vol. 11, no. 4, p. 233, 2002.

[8] K. L. Van Buren, J. M. Canfield, F. M. Hemez, and J. A. Sauer, 2012, *Code Verification of the HIGRAD computational fluid dynamics solver*, (Publication No. LA-UR-12-21165), Los Alamos National Laboratory.

[9] M. A. Finney, 1998, *FARSITE: Fire area simulator-model development and evaluation*, (Publication No. RMRS-RP-4), USDA Forest Service, Rock Mountain Station.

[10] J. Coen, M. Cameron, J. Michalakes, E. Patton, P. Riggan, and K. Yedinak, "WRF-FIRE: Coupled weather-wildland fire modelling with the weather research and forecasting model," *Journal of Applied Meteorology and Climatology*, vol. 52, no. 1, pp. 16-38, 2013.

[11] J. Coen, 2013, *"Modeling wildland fires: A description of the coupled atmosphere-wildland fire environment model (CAWFE),"* NCAR Earth System Laboratory.

[12] C. C. Simpson, J. J. Sharples, and J. P. Evans, "Resolving vorticity-driven lateral fire spread using the WRF-FIRE coupled atmosphere-fire numerical model," *Natural Hazards and Earth System Sciences*, vol. 14, no. 9, pp. 2359-2371, 2014.

[13] A. J. Chorin and J. E. Marsden, *A Mathematical Introduction to Fluid Mechanics*, Springer Science and Business Media, 2013.

[14] M. J. Harris, "Chapter 38. Fast Fluid Dynamics Simulation on the GPU," in *GPU Gems*, NVIDIA Corporation.